

# Preparation, Characterization And Nanozymes Activity Of ZnO And SnO<sub>2</sub> Nanoparticles

Alaa A. MAJEED<sup>1</sup>, Rashed T. RASHEED<sup>1\*</sup>

<sup>1</sup>Applied Chemistry Division, School of Applied Science, University of Technology, Baghdad, Iraq.

ORCID iDs: Rashed Taleb Rasheed, <https://orcid.org/0000-0002-7685-5377>

---

## Abstract

Different nanoparticles zinc oxide (ZnO), and tin dioxide (SnO<sub>2</sub>) were prepared by different methods (autoclave and sol-gel). The nanoparticles were annealed at different temperatures (90°C and 400°C). The structures and surface morphology were characterized by Uv/Visible and FT-IR measurements, x-ray diffraction (XRD), Atomic Force Microscope (AFM), and Scanning Electron Microscopy (SEM). The nanozymes (enzyme mimetic) activity as Catalase (CAT), and Peroxidase (Pxase) were measured. The results of nanozymes activity showed there is a maximum activity as CAT for ZnO (90°C) while there is a maximum activity as Pxase for SnO<sub>2</sub> (90°C), and there are decreasing in the activity for both nanoparticles when annealed at 400°C.

**Keywords:** Zinc oxide, tin dioxide, catalase, peroxidase, nanozyme

---

## 1. Introduction

Scientists are interested in nanomaterials and nanocomposites because of their unique magnetic, chemical, optical, and electrical characteristics, which make them useful for a variety of applications, such as catalysts [1], chemical sensors [2], gas sensors [3], antibacterial activity [4], and colorimetric sensors [5]. Nanoparticles in the size range of 100 nm have become a focus of research and concern in recent years. Because of their safety and stability, inorganic metal oxides (TiO<sub>2</sub>, MgO, CaO, and ZnO) are studied as antibacterial agents. The minimum antibacterial activity of ceramic powders has been investigated using methods such as indirect conductometric tests [6]. ZnO is a material having a direct bandgap (3.37 eV) [7] at room temperature, a high exciton binding energy (60 meV), and good chemical stability. It has a hexagonal structure with  $a = b = 3.250$  and  $c = 5.206$  lattice constants [8]. Because of their characteristics and uses, SnO<sub>2</sub> nanostructures have become one of the most significant oxide

nanostructures[9]. Tin oxide ( $\text{SnO}_2$ ) is one of the most promising n-type wide bandgap semiconducting materials among metal oxides (3.6 eV)[10]. Different methods can be used to make zinc oxide nanoparticles which include the sol-gel method [11], chemical vapor deposition, thermal decomposition, and thermal evaporation process[12], and preparation methods of  $\text{SnO}_2$  nanoparticles are similar to  $\text{ZnO}$  nanoparticles chemical vapor deposition, the sol-gel method, and thermal evaporation of oxide powders[13]. The applications that have been used for nano-oxides are imitating enzyme action such as vanadium oxide, cerium oxide, and manganese oxide[14]. At ambient temperatures, nanozymes are a subgroup of nanoparticle-based catalysts that catalyze enzyme-like processes. Nanozymes are appealing not just because of their great stability and inexpensive cost, but also because they may be used to explore basic processes at nanoscale surfaces. Many nanoparticles have oxidase, peroxidase, and/or catalase-like activities, such as gold, graphene oxide, and other metal oxides. It's worth noting that while numerous peroxidase nanozymes have been described (those that use  $\text{H}_2\text{O}_2$  as a substrate), only a handful exhibit oxidase activity[15]. Catalase (CAT) is a metalloprotein that is present in all oxygen-consuming organisms [16]. Catalase activity in blood is nearly exclusively attributed to erythrocytes since this enzyme is soluble in erythrocytes and human erythrocytes are generally rich in catalase[17-19]. peroxidase is a heme-containing enzyme that oxidizes a wide range of organic and inorganic substances using hydrogen peroxide[11].

In this work, we prepared nanoparticles ( $\text{ZnO}$  and  $\text{SnO}_2$ ) in different methods and measured the enzymatic activity (Catalase and peroxidase).

## **2. Experimental**

### **2.1 Materials**

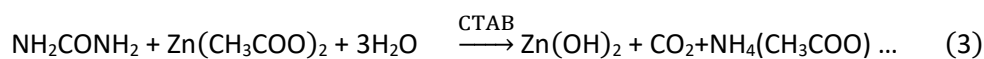
Ammonium hydroxide ( $\text{NH}_4\text{OH}$ ), Zinc acetate  $\text{Zn}(\text{OAc})_2$  and Tin chloride ( $\text{SnCl}_2 \cdot 2\text{H}_2\text{O}$ ) were purchased from Sigma (Sigma-Aldrich, Taufkirchen, Germany). Urea ( $\text{NH}_2\text{CONH}_2$ ) was purchased from (Merck, Germany), Cetyltrimethyl ammonium bromide (CTAB) was purchased from (BDH) and hydrogen peroxide ( $\text{H}_2\text{O}_2$ ) was purchased from (Chem-lab).

### **2.2 Methods**

#### **2.3 Preparation of zinc oxide nanoparticles (ZnO NPs)**

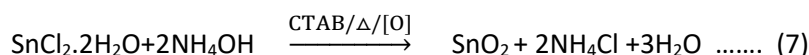
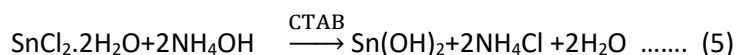
The hydrothermal method (autoclave) was used to prepare zinc oxide nanoparticles, with minor modifications [12,20]. Zinc acetate ( $\text{Zn}(\text{CH}_3\text{COO})_2$ ), urea ( $\text{NH}_2\text{CONH}_2$ ), and cetyltrimethylammonium bromide (CTAB) are used in the following processes, dissolve 3 g zinc acetate, 1.25 g urea, and 0.5 g CTAB in 50 ml distilled water, stirring continually until completely dissolved. Then place it in an autoclave and

heat it at 200° C for 6 hours. When the reaction is finished, the precipitate should be washed three times to remove any impurities, then dried at 90° C for 60 minutes and annealed at 400°C for 120 minutes, as shown in the equations.



#### 2.4 Preparation of tin dioxide nanoparticles (SnO<sub>2</sub> NPs):-

The sol-gel method was used to make tin dioxide nanoparticles, as described in reference [21]. Tin chloride (SnCl<sub>2</sub>·2H<sub>2</sub>O), cetyltrimethylammonium bromide (CTAB), and ammonium hydroxide (NH<sub>4</sub>OH) were employed, with the first step consisting of dissolving (3 gm.) of tin (II) chloride in distilled water (50 ml) and then adding (0.5 gm.) of cetyltrimethylammonium-ammonium bromide (CTAB). Ammonium hydroxide in distilled water at a ratio of (1:10) was titrated with the above solution until the reaction was complete (the solution became alkaline pH ≈ 8). Then it was dried for 60 minutes at 90°C before being annealed at 400°C for 120 minutes, the equations were explained as follows:



### 3. Enzyme measurements

#### 3.1 Catalase (CAT) mimetic activity measurements

Catalase (CAT) mimetic activity measurements were used absorbance by the Uv/Visible spectrometer method at a wavelength of 240 nm as the following procedure: three containers (50 mL) labels as (T, C, and B) to every nanoparticle (ZnO and SnO<sub>2</sub>). A weight (0.001g) and (0.002 g) of (ZnO and SnO<sub>2</sub>) respectively were added to both T and B containers. Two and one milliliters of buffer phosphate (50 mM, pH = 7) were added to C, B and T containers respectively. One milliliter of hydrogen peroxide (2.8 mM) was added to both T and C containers. All containers were shaking for 5 minutes, on the

shaker. Measuring the absorbance of each container by the Uv/Visible spectrometer at a wavelength of 240 nm. The following equation was used to determine catalase mimic activity based on first-order reaction [22]

$$\text{Catalase mimic activity (K)} = (2.303 / t) \log (C_0 / C) \dots\dots (8)$$

Where (t) is the reaction time in minutes.  $C_0$  and C are the concentrations of  $H_2O_2$  in the cell reaction before and after the reaction, respectively, C is equal to  $(C_1 - T_1)$ .

### 3.2 Peroxidase mimetic activity measurements

Peroxidase mimetic activity measurements were used by the Uv/Visible spectrometer method at a wavelength of 292 nm for zinc oxide and tin dioxide as the following procedure: three containers (50 mL) labels as (T, C, and B) to every nanoparticle (ZnO and  $SnO_2$ ). A weight (0.012g) of (ZnO and  $SnO_2$ ) were added to both T and B containers. 4.95 mL and 5 mL of buffer phosphate (50 mM, pH = 7.2) were added to T, C, and B containers respectively. 0.05 ml of orthophenylenediamine (OPD) was added to C and T containers. Then one milliliter of hydrogen peroxide (2.8 mM) was added to all containers. All containers were shaking for 5 minutes, on the shaker. Measuring the absorbance of each container by the Uv/Visible spectrometer at a wavelength of 292 nm. The following equation was used to determine peroxidase mimic activity [23].

$$U/t \text{ min} = [C - (T - B)] (\text{Vol}/\text{Wt})/t \text{ min} \dots\dots (9)$$

Where; B = blank, C = control, T = test, Vol. = total volume of solution reaction, and Wt. = weight of nanoparticles in container. t = the reaction time after 45 minutes

## 4. Results and discussion

### 4.1 Optical properties of the nanoparticles solutions.

The optical characteristics of nanoparticle solutions (about  $1 \times 10^{-5}$  M) were produced by dissolving the metal oxides in ethanol. Figure (1) shows the optical prosperity (transmittance) of metal oxides at various temperatures (90 °C and 400 °C) between region 250 nm to about 550 nm

#### 4.1.1 The spectrum of ZnO nanoparticles

The spectrum of ZnO nanoparticles as-prepared display a small drop in transmittance edge (blue shift) from 370 nm to 366 nm with increasing annealing temperatures to 400°C, as seen in figure(1), resulting in optical transmittance and attributed to structural homogeneity and particle crystallization. The following equation can be used to calculate the value of the energy gap [24].

$$\text{Energy gap (eV)} = 1240/\lambda_{\text{max}} \dots\dots\dots (10)$$

Where 1240 is the factor used to convert nm to eV and  $\lambda_{\text{max}}$  is the maximum transmittance in nm.

According to equation (7) and the results of figure (1), the energy gap of ZnO as-prepared is 3.35eV and that of annealing at 400 °C is 3.38eV, this result agrees with the reference

#### **4.1.2 The spectrum of SnO<sub>2</sub> nanoparticles**

The optical transmission of SnO<sub>2</sub> (as-prepared) nanoparticles shows a small rise in the transmittance edge (redshift) with increasing annealing temperature from 366 nm to 372 nm, which is related to an increase in orientation and may be attributable to heat treatment that increases the mobility of atoms in rearrangement processes within the lattice. As a result and equation (7), the energy gap of SnO<sub>2</sub> as-prepared is 3.38 eV, while that of SnO<sub>2</sub> annealing at 400 °C is 3.33 eV, this result agrees with the reference [25].

### **4.2 Fourier Transform infrared (FT-IR) analysis**

#### **4.2.1 FTIR Spectra for Zn(OH)<sub>2</sub> and ZnO nanoparticles**

FTIR spectra spectrum of Zn (OH)<sub>2</sub> nanoparticles, figure (2-a), show two bands at 3305 cm<sup>-1</sup> refer to O-H bond vibrations stretching [26]. The peak at 468 cm<sup>-1</sup> relates to Zn-O bonding [27]. While the weak vibrations at 1506 cm<sup>-1</sup>, and 1010 cm<sup>-1</sup> corresponds to the stretching C=O, and C-O for acetate [28]. FTIR spectra spectrum of ZnO nanoparticles, figure (2b), show two bands at 3461 cm<sup>-1</sup> and 1606 cm<sup>-1</sup> are refer to O-H bond vibrations stretching and bending of water respectively. Meanwhile, the peak at 565 cm<sup>-1</sup> corresponds to the stretching Zn-O mode, indicating the synthesis of ZnO[29].

#### **4.1.2 FTIR Spectra for Sn(OH)<sub>4</sub> and SnO<sub>2</sub> nanoparticles**

FTIR samples of Sn(OH)<sub>4</sub> nanoparticles figure (2-c), show peaks at 3396 cm<sup>-1</sup> and 1639 cm<sup>-1</sup> attributed to a surface-absorbed hydroxyl group[30, 31]. The stretching and flexing vibrations were given for bands at 2922 cm<sup>-1</sup>, 2852 cm<sup>-1</sup> relate to the organic trace residues of the CTAB surfactant were ascribed to these C-H peaks [32]. The NH deformation of ammonia and the NH vibration of deforming the ammonium hydroxide has been attributed to the peak at about 1470 cm<sup>-1</sup>, SnO<sub>2</sub> stretching modes Sn-O-Sn and Sn-OH, respectively, were ascribed to bands of 665 and 554 cm<sup>-1</sup> figure (2) [33]. FTIR samples of SnO<sub>2</sub> nanoparticles figure (2-d), show peaks at 3421 cm<sup>-1</sup> and 1635 cm<sup>-1</sup> attributed to a surface-absorbed hydroxyl group. The smallest strips at 578 cm<sup>-1</sup> and 559 cm<sup>-1</sup> ascribed to Sn-O strip are the most significant absorbents identified after thermal bonding [34].

### 4.3. X-Ray Diffraction (XRD)

X-ray Powder Diffraction (XRD) to determine their crystal structure was performed using an X-ray diffractometer with  $\text{Cu K}\alpha$  radiation ( $\lambda = 1.5418 \text{ \AA}$ ) in the range ( $20\text{--}80^\circ$ ).

#### 4.3.1. The X-Ray Diffraction for $\text{Zn(OH)}_2$ and $\text{ZnO}$ nanoparticles

X-Ray Diffraction patterns of zinc oxide nanoparticles as prepared is similar to X-ray diffraction (XRD) the crystallinity of annealed  $\text{ZnO}$  nanoparticles. The XRD spectra of  $\text{ZnO}$  nanoparticles as prepared see Fig. (3-a) (No. JCPDS Card 008, 82-1042 and 5-0664)[35]. The typical X-ray diffraction (XRD) patterns of annealed  $\text{ZnO}$  nanoparticles are seen in Fig(3-b) All of the observed XRD patterns included well-defined diffraction reflections at  $2\theta = 31.5^\circ, 34.4^\circ, 36.1^\circ, 47.6^\circ, 56.5^\circ, 62.9^\circ, 66.3^\circ, 68.1^\circ, 69.3^\circ$ , which corresponded to the wurtzite hexagonal phase  $\text{ZnO}$  lattice planes of (100), (002), (101), (102), (110), (103), (200), (112)[29]. The lattice constants ( $a = b = 3.229 \text{ \AA}$  and  $c = 5.175 \text{ \AA}$ ,  $c/a = 1.602$ ) and diffraction peaks corresponding to the planes (100), (002), (101), (102), (110), (103) obtained from X-ray diffraction data are consistent with the JCPDS data of  $\text{ZnO}$

#### 4.3.2. The X-Ray Diffraction for $\text{Sn(OH)}_2$ and $\text{SnO}_2$ nanoparticles

The X-ray findings of  $\text{SnO}_2$  heated at  $90^\circ\text{C}$  are extremely comparable to the  $400^\circ\text{C}$  radiation result (JCPDS 77-0452). The obtained lattice constant  $a = 4.759 \text{ \AA}$  and  $c = 3.201 \text{ \AA}$  indicate the nanocrystal belongs to the tetragonal system. As in figure (3-c).

$$1/d_{hkl}^2 = (h^2 + k^2)/a^2 + l^2/c^2 \quad \text{----- (12)}$$

The XRD patterns of  $\text{SnO}_2$  particles shows polycrystalline phases and is compared with (JCPDS card no. 41-1445), the patterns display four diffraction peaks at ( $2\theta = 26.58, 33.88, 38.18, 51.90^\circ, 65.42^\circ$  and  $76.610$ ) that correspond to the diffraction planes (110), (101), (200), (211), (301) and (321) respectively[36]. As in figure (3-d) and table (1).

### 4.4. Surface Morphology by Scanning Electron Microscopy (SEM) and Energy Dispersive X-Ray Analysis (EDX).

The surface morphology image SEM with magnification at (100 nm) and its EDX results of the metal oxides ( $\text{ZnO}$  and  $\text{SnO}_2$ ) nanoparticles produced by hydrothermal technique and annealed to  $400^\circ\text{C}$  for 120 minutes. The SEM images morphology of  $\text{ZnO}$  nanoparticles, figures (4- a), demonstrate the nanoparticle aggregation is and the samples synthesized as nanoflakes. The binding energies of O and Zn are displayed as peaks in the  $\text{ZnO}$  EDX spectrum figure (4-b) at 0.55, 1.0, and 8.6 keV, respectively. And the SEM images of tin dioxide nanoparticles synthesized by sol-gel method figure (4-c). The shape

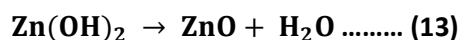
seems clustered foam-like, with tiny agglomerations of SnO<sub>2</sub> nanoparticles. While figure (4-d) represents the EDX spectrum of SnO<sub>2</sub> nanoparticles which confirms the produced are composed of Sn and O are displayed as the peak at 3.5, 4.0, 0.5 keV, respectively.

#### 4.5. Surface Morphology

AFM results of nanoparticles (ZnO and SnO<sub>2</sub>) in three (3D) dimension images and Granularity accumulation distribution charts with different temperatures: (a) as-prepared (90 °C), and (b) 400 °C,

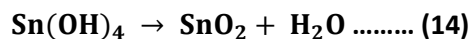
##### 4.5.1 AFM of Zinc oxide nanoparticles

Threediminutions and distribution accumulation of zinc oxide nanoparticles convert from the oval shape (figure 5-a) to a small conical shape (figure 5-b). This relates to converting the hydroxides (Zn(OH)<sub>2</sub>) to oxides (ZnO) when heating at a high temperature (400 °C). At the same time the average grain size decreases a little from 77.99 nm (as-prepared) to 72.00 nm (annealing), as in table (2) the decrease in the size may be due to converting of hydroxide to oxide form according to the following equation:



##### 4.5.2 AFM of Tin dioxide nanoparticles

Three diminutions and distribution and accumulation of tin dioxide nanoparticles convert from balls shape (figure 5-c) to smaller shape (figure 5-d). This relates to converting some of the hydroxides (Sn(OH)<sub>4</sub>) to oxides (SnO<sub>2</sub>) when heating at a high temperature (400 °C). The average grain size decreases a little from 91.49 nm (as-prepared) to 88.10 nm (annealing), as in table (2), the little decrease in the size may be due to converting of hydroxide to oxide form according to the following equation:



### 5. Applications

#### 5.1 Catalase Mimetic Activity

The mimic activities of our produced nanoparticles as Catalase in phosphate buffer solution (50Mm, pH=7.0) by employing a concentration of H<sub>2</sub>O<sub>2</sub> were measured spectrophotometrically using the extinction coefficient of 40 M<sup>-1</sup>.Cm<sup>-1</sup> at 240 nm [37].The Catalase mimetic activity was determined by the equation(8).

The results demonstrate that the catalase mimetic activities of nanoparticles change depending on the kind of nanoparticle and the degree of heating. The highest catalase mimetic activity of the nanoparticles (as-prepared) relates to ZnO while the lowest activity relates to SnO<sub>2</sub>. The sequence of

these mimetic activities was followed by the following arrangement ( $\text{ZnO} > \text{SnO}_2$ ). On the other hand, the lowest Catalase mimetic activity of the nanoparticles (annealing) relates to ZnO while the higher activity relates to  $\text{SnO}_2$ . The sequence of these mimetic activities was followed by the following arrangement ( $\text{SnO}_2 > \text{ZnO}$ ), as in figure (6) and table (3).

#### 4.2 Peroxidase Mimics Activity

The mimetic activities of our produced nanoparticles as peroxidase in phosphate buffer solution (50 mM, pH= 7.2), utilizing the reference[30], with minor modification by employing spectrophotometric technique at the wavelength ( $\lambda = 292 \text{ nm}$ ), including the use of orthophenylenediamine solution as an indicator, The equation (9) was used to calculate the peroxidase mimetic activity. The mimetic activities of nanoparticles as peroxidase were varying depending on the nanoparticle type and the degree of heating. The nanoparticles with the highest peroxidase-mimicking activity (as prepared) are  $\text{SnO}_2$ , while the nanoparticles with the lowest activity are ZnO. The simulation activity was organized in the following order: ( $\text{SnO}_2 > \text{ZnO}$ ). The nanoparticles with the highest peroxidase-mimicking activity (annealing) are ZnO, while the particles with the lowest activity are  $\text{SnO}_2$ . The simulation activity was arranged in the following order ( $\text{ZnO} > \text{SnO}_2$ ) exactly the opposite of the prepared as shown in figure (7) and table (4).

The very high decrease in the mimetic activity of  $\text{SnO}_2$  nanoparticles (annealing) from  $5.800 \text{ U/min}^{-1}$  to  $0.307 \text{ U/min}^{-1}$  despite convergence in average grain size between both samples (91.49 nm and 88.10 nm) respectively, as in table (4), maybe due to higher activity of hydroxide form ( $\text{Sn(OH)}_4$ ) form as-prepared compare with oxide form ( $\text{SnO}_2$  annealing form). On the other hand, the increased peroxidase mimetic activity of  $\text{Zn(OH)}_2$  nanoparticles is more than ZnO as in table (3), although the size of the annealing nanoparticles are smaller than that of as-prepared this indicates that there is no relationship to size in this mimetic activity.

#### Conclusion

Different methods (autoclave and sol-gel) were used to prepare ZnO and  $\text{SnO}_2$  nanoparticles respectively. Both nanoparticles were annealed at  $400 \text{ }^\circ\text{C}$  for 2 hours. Then catalase and peroxidase mimetic activities were determined against  $\text{H}_2\text{O}_2$  and OPD as substrate. The results indicated that the as-prepared of both nanoparticles were the highest as peroxide mimetic activity. While ZnO annealing at  $400 \text{ }^\circ\text{C}$  has the highest catalase mimetic activity compared with as-prepared.

#### Acknowledgement

We are thankful for university of technology Iqam and all laboratory staff who gave us assistance in the measurements.

## Reference

- [1] R. M. Tripathi and S. J. Chung, "Reclamation of hexavalent chromium using catalytic activity of highly recyclable biogenic Pd(0) nanoparticles," *Scientific Reports* 2020;10(1):, 1–14. doi: 10.1038/s41598-020-57548-z.
- [2] S. AL-Algawi, R.T. Rasheed, and S. Z. Tareq. Development of NO<sub>2</sub> gas sensor using Sn- doped ITO nanoparticles prepared by Sol-Gel method. *Engineering and Technology Journal* 2015; 33B(6):984-993, 2015..
- [3] R. J . Halbos, S. AL-Algawi, and R.T. Rasheed Gas Sensitivity of ITO Composite Prepared by Sol-Gel Method. *Engineering and Technology Journal* 2017; 35A(10): 981-986.
- [4] Z. A. Husain, A. A. Majeed, R. T. Rasheed, H. S. Mansoor, and, N. N. Hussein. (2021). Antibacterial activity of In<sub>2</sub>O<sub>3</sub> nanopowders prepared by hydrothermal method. *Materials Today: Proceedings* 2020; 42: 1816–1821, doi:10.1016/j.matpr.2020.12.189.
- [5] R. M. Tripathi and S. J. Chung, "Eco-friendly synthesis of SnO<sub>2</sub>-Cu nanocomposites and evaluation of their peroxidase mimetic activity," *Nanomaterials* 2021; 11(7): 1–13, 2021, doi: 10.3390/nano11071798.
- [6] D. Sharma, J. Rajput, B. S. Kaith, M. Kaur, and S. Sharma, "Synthesis of ZnO nanoparticles and study of their antibacterial and antifungal properties," *Thin Solid Films* 2010; 519(3): 1224–1229. doi: 10.1016/j.tsf.2010.08.073.
- [7] P. M. Aneesh, K. A. Vanaja, and M. K. Jayaraj, "Synthesis of ZnO nanoparticles by hydrothermal method," *Nanophotonic Materials IV* 2007; 6639: 66390J. doi: 10.1117/12.730364.
- [8] M. Kahouli, A. Barhoumi, A. Bouzid, A. Al-Hajry, and S. Guermazi, "Structural and optical properties of ZnO nanoparticles prepared by direct precipitation method," *Superlattices and Microstructures* 2015; 85: 7–23. doi: 10.1016/j.spmi.2015.05.007.
- [9] G. E. Patil, D. D. Kajale, V. B. Gaikwad, and G. H. Jain, "Preparation and characterization of SnO<sub>2</sub> nanoparticles by hydrothermal route," *International Nano Letters* 2012; 2(1): 2–6. doi: 10.1186/2228-5326-2-17.
- [10] S. Asaithambi, P. Sakthivel, M. Karuppaiah, R. Murugan, R. Yuvakkumar, and G. Ravi, "Preparation of SnO<sub>2</sub> Nanoparticles with Addition of Co Ions for Photocatalytic Activity of Brilliant Green Dye Degradation," *Journal of Electronic Materials* 2019; 48(4): 2183–2194. doi: 10.1007/s11664-019-07061-5.
- [11] M. Vafaei and M. S. Ghamsari, "Preparation and characterization of ZnO nanoparticles by a novel sol-gel route," *Materials Letters* 2007; 61(14–15): 3265–3268. doi: 10.1016/j.matlet.2006.11.089.

- [12] H. S. Wasly, M. S. Abd El-Sadek, and M. Henini, "Influence of reaction time and synthesis temperature on the physical properties of ZnO nanoparticles synthesized by the hydrothermal method," *Applied Physics A* 2018; 124(1): 76.
- [13] M. G. Thakare, C. G. Dighavkar, A. V Borhade, and J. S. Aher, "Synthesis , Characterization and Application of SnO<sub>2</sub> Nanoparticles," *International Journal of Recent Trends in Engineering and Research* 2016; 114–124.
- [14] H. Wei, and E. Wang, E. (2013). Nanomaterials with enzyme-like characteristics (nanozymes): next-generation artificial enzymes. *Chemical Society Reviews*, 42(14), 6060. doi:10.1039/c3cs35486e
- [15] B. Liu, Z. Huang, and J. Liu, "Boosting the oxidase mimicking activity of nanoceria by fluoride capping: Rivaling protein enzymes and ultrasensitive F<sup>-</sup> detection," *Nanoscale* 2016; 8(28): 13562–13567. doi: 10.1039/c6nr02730j.
- [16] R. T. Rasheed, H. S. Mansoor, and, A. S. Mansoor. New colorimetric method to determine catalase mimic activity. *Materials Research Express* 2020; 7(2): 025405. doi:10.1088/2053-1591/ab706b.
- [17] I. Fridovich and B. Freeman, "Antioxidant defenses in the lung," *Annual review of physiology* 1986; 48(1): 693–702.
- [18] R. T. Rasheed, H. S. Mansoor, R. R. Al-Shaikhly, T. A. Abdullah, A. D. Salman, and T. Juzsakova,. Synthesis and catalytic activity studies of  $\alpha$ -MnO<sub>2</sub> nanorods, rutile TiO<sub>2</sub> and its composite prepared by hydrothermal method. 2<sup>nd</sup> International Conference on Materials Engineering and Science (IConMEAS 2019)2020. doi:10.1063/5.0000228 .
- [19] R. T. Rasheed, H. S. Mansoor, T. A. Abdullah, T. Juzsakova, N. Al-Jammal, A. D. Salman, and T. A. Abdulla,. Synthesis, characterization of V<sub>2</sub>O<sub>5</sub> nanoparticles and determination of catalase mimetic activity by new colorimetric method. *Journal of Thermal Analysis and Calorimetry*2020. doi:10.1007/s10973-020-09725-5
- [20] N. C. Veitch, "Horseradish peroxidase: A modern view of a classic enzyme," *Phytochemistry* 2004; 65(3): 249–259. doi: 10.1016/j.phytochem.2003.10.022.
- [21] M. Aziz, S. S. Abbas, and W. R. W. Baharom, "Size-controlled synthesis of SnO<sub>2</sub> nanoparticles by sol–gel method," *Materials Letters* 2013; 91: 31–34.
- [22] H. Aebi, *Methods in Enzymology*, Catalase in vitro 1984; 105: 121–126. doi.org/10.1016/S0076-6879(84)05016-3.
- [23] S. Fornera, and P. Walde..Spectrophotometric quantification of horseradish peroxidase with o-phenylenediamine. *Analytical Biochemistry* 2010; 407(2): 293–295. doi:10.1016/j.ab.2010.07.034
- [24] S. Algawi, R. Rasheed, and H. Mansoor, "Preparation, Structural and Optical Properties of SnO<sub>2</sub>

- Thin Films Prepared by Sol-Gel Method," Asian Journal of Materials Chemistry 2017; November: 2–7. doi: 10.14233/ajmc.2017.AJMC-P33.
- [25] M. N. Zafar, Q. Dar, F. Nawaz, M. N. Zafar, M. Iqbal, and M. F. Nazar, "Effective adsorptive removal of azo dyes over spherical ZnO nanoparticles," Journal of Materials Research and Technology 2019; 8(1): 713–725. doi: 10.1016/j.jmrt.2018.06.002.
- [26] S. C. Singh, "Effect of oxygen injection on the size and compositional evolution of ZnO/Zn(OH)<sub>2</sub> nanocomposite synthesized by pulsed laser ablation in distilled water," Journal of Nanoparticle Research 2011; 13(9): 4143–4152.
- [27] Y. T. Jayarambabu, N., Kumari, B. S., Rao, K. V., and Prabhu, "Germination and growth characteristics of mungbean seeds (*Vigna radiata* L.) affected by synthesized zinc oxide nanoparticles. International Journal of Current Engineering and Technology" 2014; 4(5): 2347–5161.
- [28] A. Umar, R. Kumar, G. Kumar, H. Algarni, and S. H. Kim, "Effect of annealing temperature on the properties and photocatalytic efficiencies of ZnO nanoparticles," Journal of Alloys and Compounds 2015; 648: 46–52.
- [29] N. Shahzad, N. Ali, A. Shahid, S. Khan, and H. Alrobei, "Synthesis of tin oxide nanoparticles in order to study its properties," Digest Journal of Nanomaterials and Biostructures 2021; 16(1): 41–49.
- [30] M. Akram, A. T. Saleh, W. A. W. Ibrahim, A. S. Awan, and R. Hussain, "Continuous microwave flow synthesis (CMFS) of nano-sized tin oxide: Effect of precursor concentration," Ceramics International 2016; 42(7): 8613–8619. doi: 10.1016/j.ceramint.2016.02.092.
- [31] K. C. Suresh, S. Surendhiran, P. M. Kumar, E. R. Kumar, Y. A. S. Khadar, and A. Balamurugan, "Green synthesis of SnO<sub>2</sub> nanoparticles using *Delonix elata* leaf extract: Evaluation of its structural, optical, morphological and photocatalytic properties," SN Applied Sciences 2020; 2(10):1–13, 2020.
- [32] M. A. Farrukh, B. T. Heng, and R. Adnan, "Surfactant-controlled aqueous synthesis of SnO<sub>2</sub> nanoparticles via the hydrothermal and conventional heating methods," Turkish Journal of Chemistry 2010; 34(4): 537–550. doi: 10.3906/kim-1001-466.
- [33] R. T. Rasheed and S. D. Al-Algawi, "Annealing Effect of SnO<sub>2</sub> Nanoparticles Prepared by the Sol-Gel Method," Journal of Advanced Physics 2016; 5(3): 236–240. doi: 10.1166/jap.2016.1262.
- [34] T. Bhuyan, K. Mishra, M. Khanuja, R. Prasad, and A. Varma, "Biosynthesis of zinc oxide nanoparticles from *Azadirachta indica* for antibacterial and photocatalytic applications," Materials Science in Semiconductor Processing 2015; 32: 55–61. doi:

10.1016/j.mssp.2014.12.053.

- [35] M. Das and S. Roy, "Preparation, characterization and properties of newly synthesized SnO<sub>2</sub>-polycarbazole nanocomposite via room temperature solution phase synthesis process," *Materials Today: Proceedings* 2019; 18: 5438–5446. doi: 10.1016/j.matpr.2019.07.573.
- [36] R. F. Beers and I. W. Sizer, "A spectrophotometric method for measuring the breakdown of hydrogen peroxide by catalase," *Journal of biological chemistry* 1952; 195(1): 133–140.
- [37] S. Fornera and P. Walde, "Spectrophotometric quantification of horseradish peroxidase with o-phenylenediamine," *Analytical Biochemistry* 2010; 407(2): 293–295. doi: 10.1016/j.ab.2010.07.034.

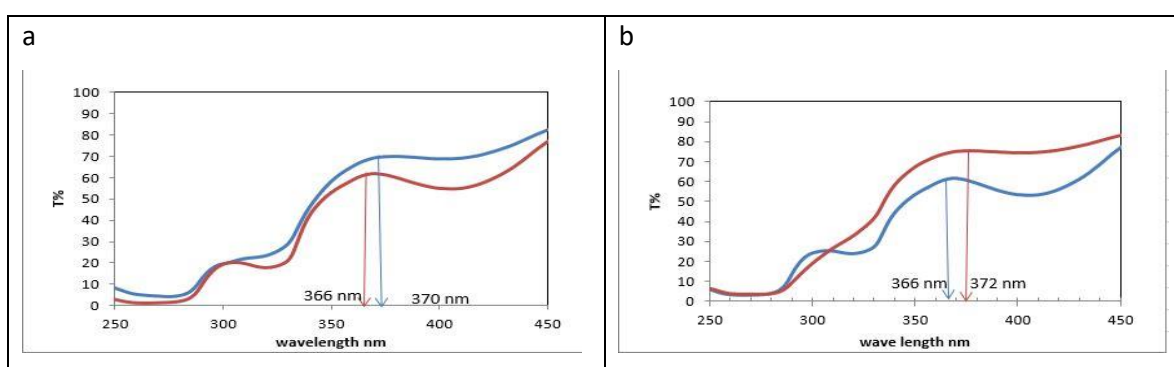
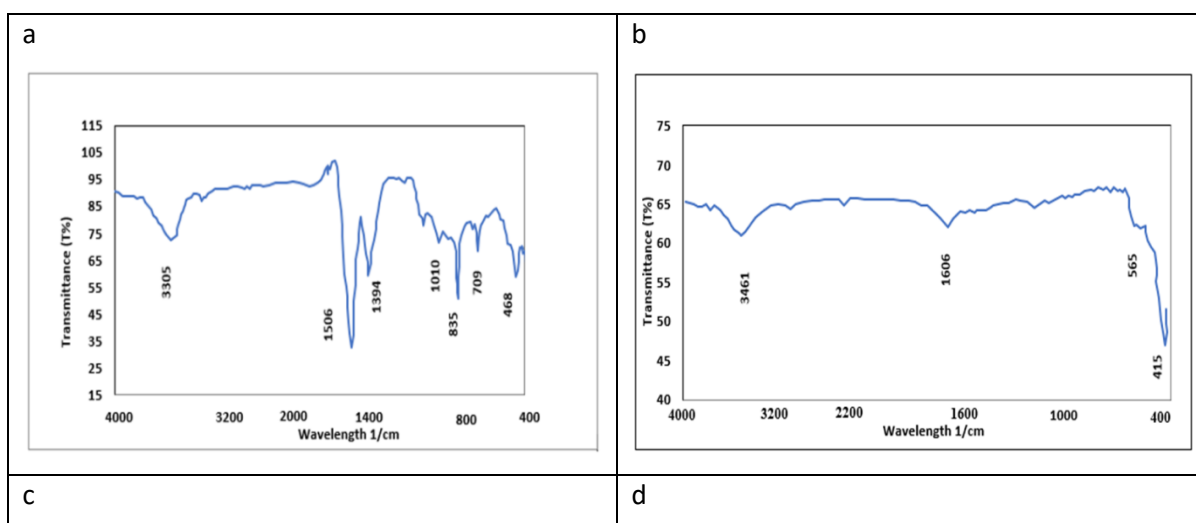


Figure (1) The optical transmittance for nanoparticles as-prepared (blue line) and annealing at 400 °C (red line) of A, ZnO NPs and B, SnO<sub>2</sub> NPs.



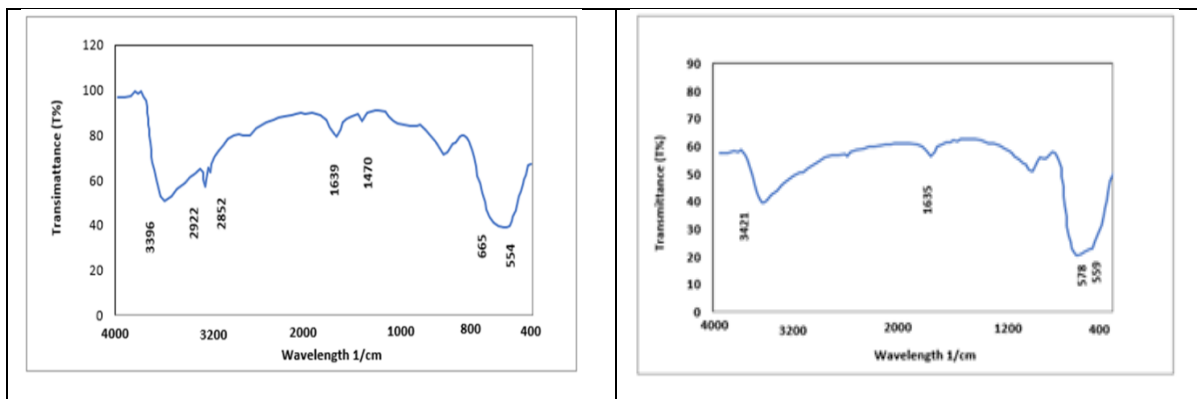


Figure (2) : FTIR Spectra for (a)  $\text{Zn(OH)}_2$  at  $90^\circ\text{C}$  for 60 min , (b)  $\text{ZnO}$  at  $400^\circ\text{C}$  for 120 min. (c)  $\text{Sn(OH)}_2$  at  $90^\circ\text{C}$  for 60 min ,(d)  $\text{SnO}_2$  at  $400^\circ\text{C}$  for 120 min.

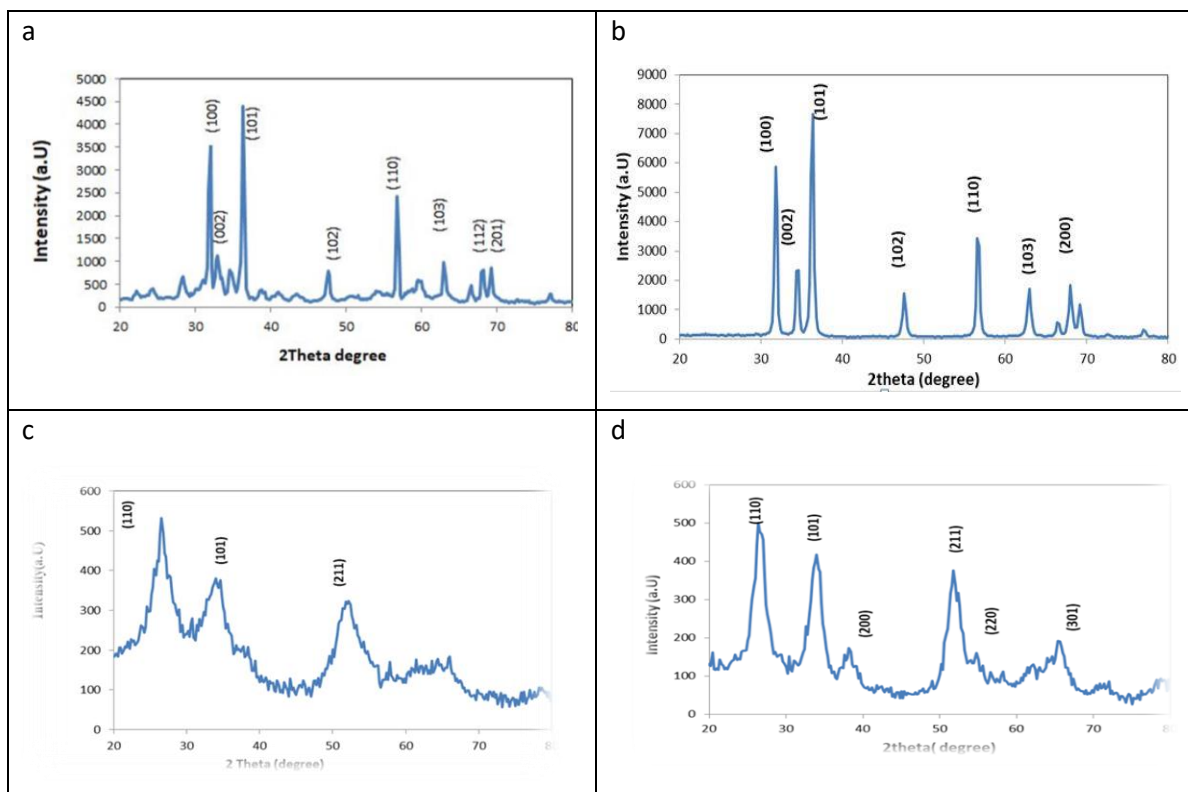


Figure (3) XRD of (a) $\text{Zn(OH)}_2$  , (b)  $\text{ZnO}$ , (c)  $\text{Sn(OH)}_2$  and  $\text{SnO}_2$  heating at  $90^\circ\text{C}$  for 60 min (a and c), annealing at  $400^\circ\text{C}$  for 120 min (b and d).

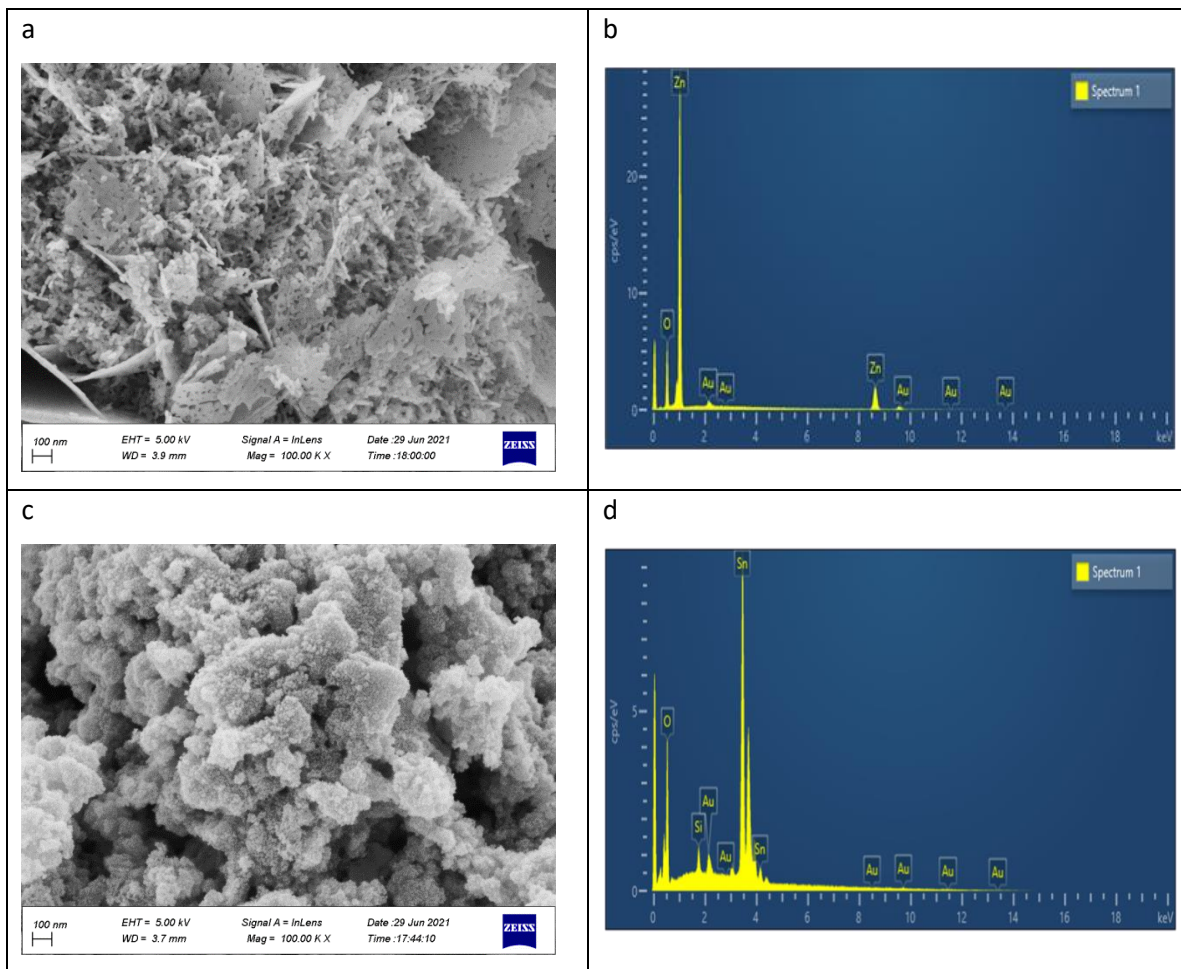
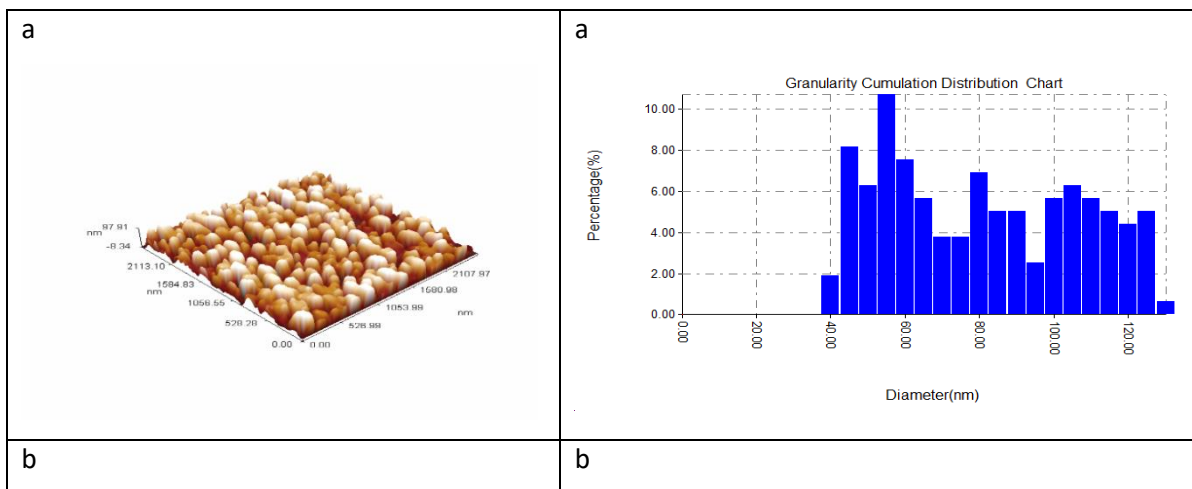


Figure (4 ) SEM image of (a) ZnO and (b) its EDX spectrum, (c) SEM image of SnO<sub>2</sub> and (d) its EDX spectrum.



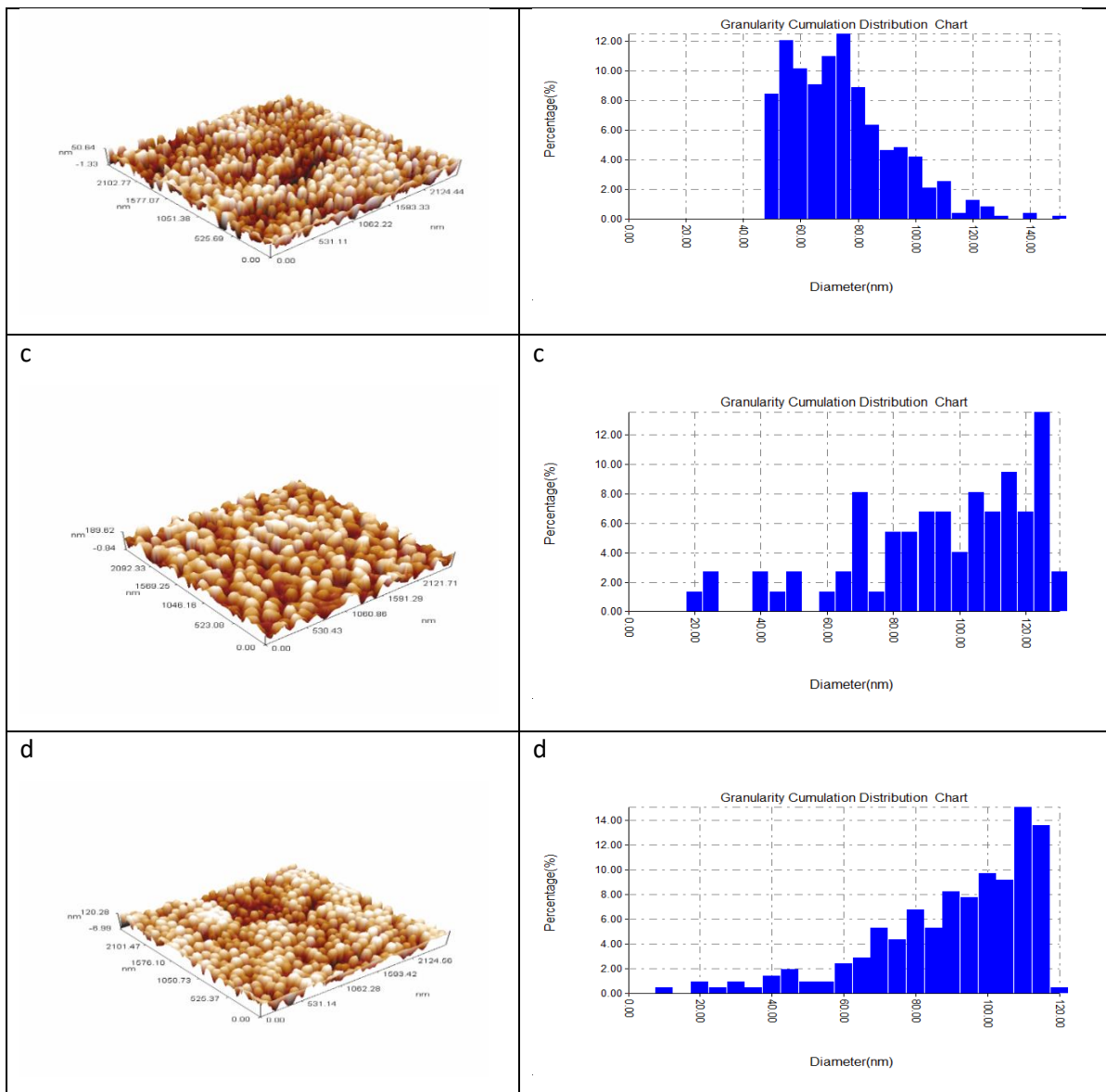


Figure (5): AFM images at 3D and Granularity accumulation distribution charts of (a) ZnO, as-prepared, (b) ZnO annealing, (c) SnO<sub>2</sub> as-prepared and (d) SnO<sub>2</sub> annealing at 400 °C for 120 min.

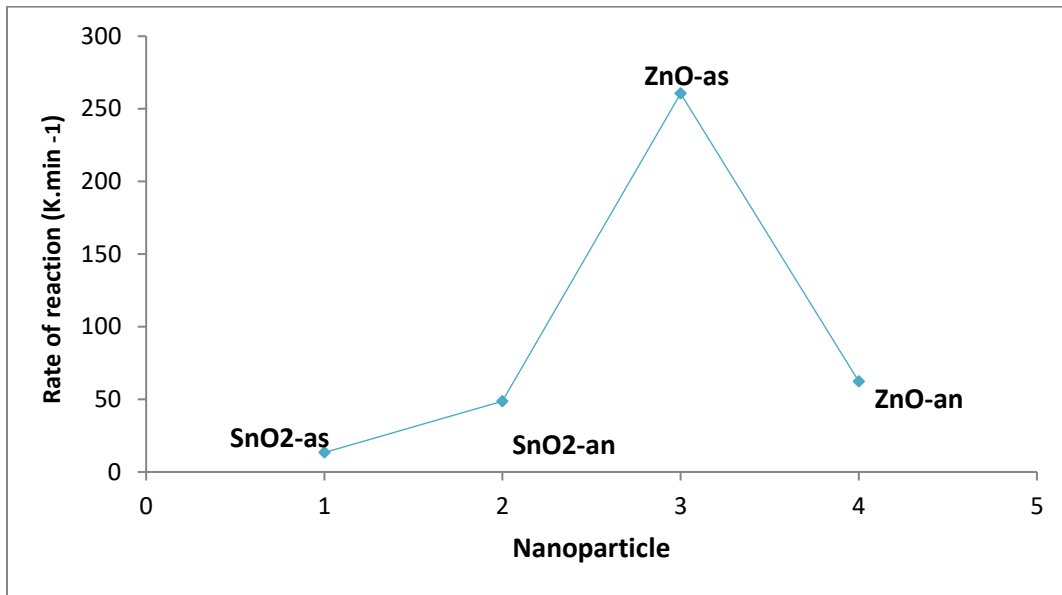


Figure: (6) Catalase mimetic activities of ZnO and SnO<sub>2</sub> at heating 90 C for 60 min and ZnO and SnO<sub>2</sub> at annealing 400 C for 120 min

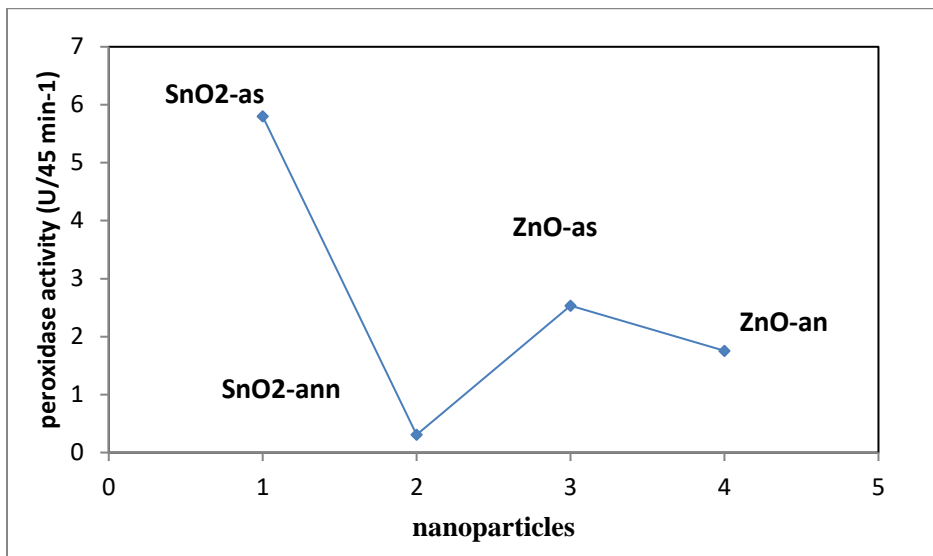


Figure (7): Peroxidase mimetic activities of ZnO, SnO<sub>2</sub> at heating 90 °C for 60 min and ZnO, SnO<sub>2</sub> at annealing 400 °C for 120 min.

Table (1): The results of the XRD for ZnO and SnO<sub>2</sub> at temperatures (90 °C, and 400 °C) for 120 min.

	2θ (deg)	hkl	FWHM (deg)	d (Å°)	D (Å°)	Lattice constant a = b (Å°)	Lattice constant c (Å°)
ZnO heating at 90 °C for 90 min	36.39	101	0.556	2.466	150.1	3.231	5.219
	31.93	100	0.569	2.799	144.9	-	-
	56.76	110	0.518	1.620	174.1	-	-
ZnO annealing at 400 °C for 120 min	36.34	101	0.576	2.469	145.0	3.238	5.205
	31.87	100	0.545	2.805	151.2	-	-
	56.66	110	0.554	1.623	162.7	-	-
SnO <sub>2</sub> at heating 90°C	26.67	110	3.461	3.339	23.573	4.7229	3.180
	52.03	211	3.716	1.756	23.772	-	-
	33.95	101	3.771	2.638	22.012	-	-
SnO <sub>2</sub> annealing at 400 °C for 120 min	26.58	110	1.950	3.350	41.85	4.7377	3.184
	33.88	101	1.970	2.643	42.12	-	-

Table (2): Average grain size of nanoparticles at (90 °C, and 400 °C) and their ionic potential.

Metal Oxide Nanoparticles	Average grain size(d) (nm) heating at		Ionic Potential (Charge/radii)
	90 °C	400 °C	
ZnO	77.99 nm	72.00 nm	0.027
SnO <sub>2</sub>	91.49 nm	88.10 nm	0.057

Table (3): CAT mimetic activity values of nanoparticles at two (90 °C and 400 °C).

Metal Oxide Nanoparticles	CAT activity (K. min <sup>-1</sup> )	
	As-prepared	Annealing
ZnO	260.56	62.29
SnO <sub>2</sub>	13.39	48.65

Table (4): Peroxidase mimetic activities of metal oxides nanoparticles at heating 90 °C for 60 min and annealing at 400 °C for 120 min.

<b>Metal Oxide Nanoparticles</b>	<b>Peroxidase activity (U/min<sup>-1</sup>)</b>	
	<b>As-prepared</b>	<b>Annealing</b>
ZnO	2.533	1.755
SnO <sub>2</sub>	5.800	0.307